

# 1 Introduction

- 1605.01735, *Machine Learning Phases of Matter*, Carrasquilla & Melko: Used supervised learning with neural-network to classify raw spin configurations into two phases for classical Ising model, square-ice model and gauged Ising model. The trained network for the square-lattice classical Ising model correctly identifies the critical temperature for triangular-lattice classical Ising model without “information about the Hamiltonian, the lattice structure, or even the general locality of interactions”. For the square-ice and gauged Ising models where there is no conventional order parameter, they are able to distinguish between the ground and high-temperature states.
- 1606.00318, *Discovering Phase Transitions with Machine Learning*, Lei Wang: Used the unsupervised methods of PCA and clustering to identify phase transitions and order parameters using raw spin configurations in classical Ising model and COP Ising model ( $\sum \sigma = 0$ ).
- 1609.02552, *Machine Learning Phases of Strongly Correlated Fermions*, Ch’ng et.al.: Used neural-network to identify phases in 3d Hubbard model of fermions on cubical lattice.
- 1610.02048, *Learning Phases of Matter by Confusion*, van Nieuwenburg et.al.: Unsupervised methods of PCA and clustering on the entanglement spectrum or Kitaev model clearly identifies different topological phases. Supervised learning with neural-network identifies phases as well, even when omitting a region around the phase-transition point. Their “confusion scheme” systematically trains on data incorrectly labelled according to a tunable parameter. Asking when the accuracy of the trained network is highest on the entire data set narrows in on the “correct” value of the parameter and thus the location of the phase transition. This scheme is applied to the classical Ising model in 2d and the random-field Heisenberg chain.
- 1703.02435, *Unsupervised learning of phase transitions: from principal component analysis to variational autoencoders*, Wetzel: Used unsupervised methods of PCA and variational autoencoder on 2d classical Ising model and 3d XY model.
- 1704.00080, *Discovering Phases, Phase Transitions and Crossovers through Unsupervised Machine Learning: A critical examination*, Hu et.al.: Used PCA and autoencoders to identify phase transitions in square and triangular Ising models, biquadratic-exchange spin-one Ising model (highly degenerate). Blume-Capel model (both first- and second-order transitions) and 2d XY model.

Some methods:

- PCA: dimensionally reduce data to hyperplane where variance is largest (principal axes).
- Autoencoder: “dimensional reduction” idea applied to neural-networks. Have a hidden layer with very few nodes and train the network to reconstruct data similar to input data based just on that hidden layer (put a bottle-neck in neural network).

# 2 TDA

For any discrete data set, persistent homology entails a sequence of simplicial complexes ( $\alpha$ , Vietoris-Rips, &c.) of varying granularity in which homological cycles first appear and then disappear. The choice in filtration corresponds to different ways to add edges and faces to the simplicial

complex as some parameter is varied. This process produces a collection of persistence data consisting of births and deaths,  $\{b_i, d_i\}$ , for each of the cycles. Persistence diagrams are a way to visualize these topologically derived data.

The persistence diagram contains information about the size of features in the data. Since such topological data are robust against small perturbations in the original data set, TDA is a useful tool in statistical analyses of many systems.

(Why persistence image is necessary... robustness against sudden appearance of cycles, small perturbations in persistence data, &c.) To create the persistence image, begin by transforming the persistence data to  $\{b_i, p_i\} = \{b_i, d_i - b_i\}$ . Each point is then smoothed, which allows for small perturbations in the topological data to have small effects. Choosing gaussians of fixed width, the full density is

$$\rho(x, y) = \sum_i w(b_i, p_i) \frac{1}{2\pi\sigma^2} \exp \left[ -\frac{(x - b_i)^2 + (y - p_i)^2}{2\sigma^2} \right] \quad (1)$$

The weighting function should be chosen so that  $w(b_i, 0) = 0$ ; this ensures that the sudden appearance of a cycle is accounted for smoothly (choice here?). The persistence image is then the vector obtained by integrating  $\rho$  over a series of “pixels” (bins):

$$I_p = \iint_p \rho(x, y) dx dy \quad (2)$$

This process can be done for  $H_0, H_1, \dots$  and the respective vectors adjoined or treated separately. Ultimately, we have now a vector in  $\mathbb{R}^n$  ( $n$  not too large!) which is a representation of the homological structure of the original data set.

### 3 Spin Models

Here we will apply the techniques of TDA to lattice spin systems. The traditional Ising model is rich in behaviour, despite being simple to describe; in two or more dimensions there is a second-order phase transition from an ordered to random state. While it is relatively easy to distinguish between these states simply by looking at the spin configurations, there exists systems in which the different states are not as readily identified. It has been demonstrated that one can use machine learning to identify phases of matter for such spin systems. We will show that this classification can also be done using persistence images built from the spin configurations, where physical characteristics of the data such as sizes of features play a central role.

As a starting point we begin with the 2d Ising model on a square lattice:

$$H = - \sum_{\langle ij \rangle} s_i s_j + h \sum_i s_i \quad (3)$$

where the sum is over all pairs of adjacent spins. Each  $s_i$  takes values in  $\{-1, 1\}$ . We will be interested in the case of no external magnetic field,  $h = 0$ .

We take as data the physical locations of spins which all point in the same direction as the majority of spins after reaching equilibrium with a thermal bath. At very low temperatures when

Figure 1: Example PD  $\rightarrow \rho \rightarrow$  PI process.

Figure 2: Example spin configurations above and below phase transition.

nearly all spins are aligned cycles are born and die very quickly, while at high temperatures features in the spins may be longer-lived.

Of interest also are spin systems in which there are topological phases, such as the  $\mathbb{Z}_2$ -gauged Ising model (see [*Gauge fields...*, Balian et.al.]). These theories enjoy a local gauge invariance which ensures that there is spontaneous magnetization at low temperatures. Rather, in dimensions  $d > 2$  the phase transition is signalled by a change in the spin-spin correlation function. For  $C$  a closed path in the lattice, at low temperature one finds a “perimeter law”,

$$\langle \prod_C s_i \rangle \sim e^{-h(\beta)L} \quad (4)$$

while at high temperatures one finds an “area law”,

$$\langle \prod_C s_i \rangle \sim e^{-f(\beta)A} \quad (5)$$

for  $L$  the length of the path  $C$  and  $A$  the minimum number of plaquettes needed to span  $C$ . The arguments which lead to these expressions do not apply in  $d = 2$  (see section V.D. of [*An introduction...*, Kogut]) as the radius of convergence for the validity of the perimeter law is zero. One may also understand the special case of  $d = 2$  as being a consequence of the equivalence

$$\left( 2d \mathbb{Z}_2\text{-gauged Ising model} \right) = \left( 1d \text{ Ising model} \right) \quad (6)$$

found by comparing the partition functions of the two models after having chosen a convenient gauge. One can, however, still hope to distinguish between high and low temperature spin configurations, as correlation lengths do change with temperature.

For  $d > 2$  we can hope to do more: not only identify high and low temperature configuration but also determine the critical temperature at which one shifts from a perimeter to area law. All of this occurs without the obvious spontaneous magnetization that is present in the 2d Ising model. (We will see if...) TDA techniques are powerful enough to pick up on this distinction in the topological ordering of the states.

## 4 Models

### 4.1 Classical Ising Model

Spins are located at the vertices of the lattice  $\mathbb{Z}^d$  and the Hamiltonian is

$$H = - \sum_{\langle i,j \rangle} s_i s_j \quad (7)$$

where  $\langle i,j \rangle$  denotes all pairs of adjacent spins. The energy per spin is  $-d$  at  $T = 0$  and 0 at  $T = \infty$ .

- 2d: Phase transition at  $T_c \approx 2.269$  from ordered to disordered. Exponential spin-spin correlation functions except for power-law at the critical point.
- 3d: Phase transition at  $T_c \approx 4.512$  from ordered to disordered. Finite  $N$ :  $T_c^{-1} \approx 0.2212 - \frac{2.4454}{N}$  (see [0406135]). Exponential spin-spin correlation functions except for power-law at the critical point.

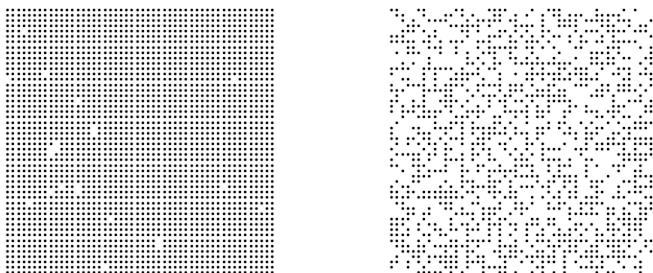


Figure 3: Example configurations for 2d Ising model at  $T = 1.5$  (left) and  $T = \infty$  (right).

## 4.2 Square Ice Model

Spins are located on the edges of the cubical lattice  $\mathbb{Z}^d$  and the Hamiltonian is

$$H = \sum_v \left( \sum_{i \in v} s_i \right)^2 \quad (8)$$

$v \in \mathbb{Z}^d$  are the vertices and  $i \in v$  is a sum over spins on edges connected to that vertex. The energy per spin is 0 at  $T = 0$  and 2 at  $T = \infty$ .

- 2d & 3d: Based on  $\langle E \rangle$ , phase transitions somewhere around  $T = 1 \rightarrow 2$ . (Find in lit?)

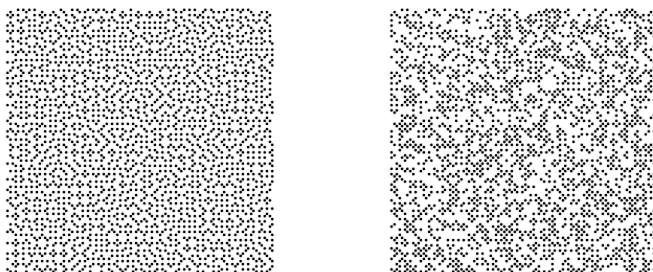


Figure 4: Example configurations for square ice model at  $T = 0$  (left) and  $T = \infty$  (right).

## 4.3 $\mathbb{Z}_2$ -gauge Ising Model

Spins are located on the edges of the cubical lattice  $\mathbb{Z}^d$  and the Hamiltonian is

$$H = - \sum_p \prod_{i \in p} s_i \quad (9)$$

$p$  are the “plaquettes” and  $i \in p$  is a product over the four spins around the edges of the face. The energy per spin is  $\frac{1-d}{2}$  at  $T = 0$  ( $dN^d$  spins and  $\binom{d}{2}N^d$  plaquettes) and 0 at  $T = \infty$ .

- 2d: No phase transition. Can still hope to classify  $T = 0$  vs  $T = \infty$ .
- 3d: No spontaneous magnetization. Phase transition at  $T_c \approx ??$  from perimeter- to area-law correlation functions. (Couldn't find value of  $T_c$  in lit... judging from  $\langle E \rangle$  seems to be around 1.)

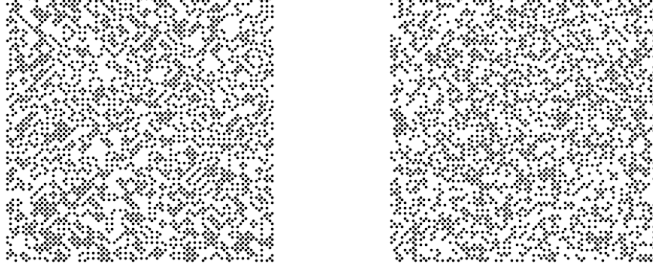


Figure 5: Example configurations for gauged Ising model at  $T = 0$  (left) and  $T = \infty$  (right).

## 5 Results

(TO DO:) Apply logreg trained on square-lattice Ising model to triangular-lattice Ising model (critical temperature is known).

(TO DO:) For  $k$ -means classification, determine best value of  $k$  (should be two!). Perhaps can show that for those models without a phase transition (e.g. 2d gauged Ising model) that  $k = 1$  is appropriate?

(TO DO:) Near  $T_c$  we expect the characteristic scale-invariance of critical phenomena to be evident in the persistence diagrams/images. By considering temperatures close to  $T_c$  we hope to find signatures of the diverging correlation length in the derived topological data.

### 5.1 2d Classical Ising Model

Used Wolff cluster algorithm to sample configurations weighted by Boltzmann factor. For each temperature in  $\{1.00, 1.05, 1.10, \dots, 3.50\}$  500 simulations were run, each washing the grid until each spin is flipped an average of 20 times.

The persistence images are characterized by a large number of short-lived 1-cycles which are born very early. The logistic regression uses the number of these cycles to classify configurations into two phases (roughly it counts the number of tiny islands of minority spins).

### 5.2 2d Square-ice Model

## 6 Discussion

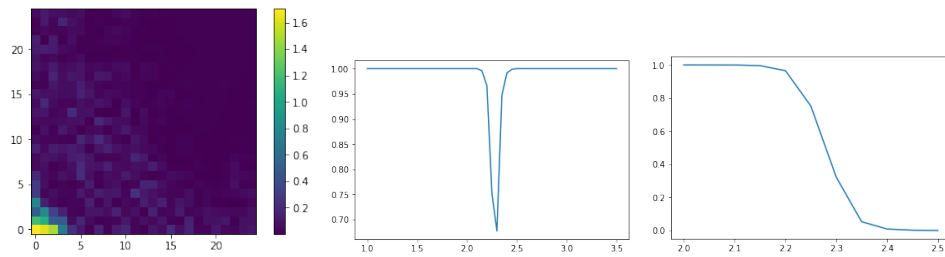


Figure 6: Left: coefficients for logreg. Center: accuracy on testing data. Right: average classification on testing data (binned). The cross-over point gives an estimate for the critical temperature,  $T_c \approx 2.2796$ .